Direct observation of imprinted antiferromagnetic vortex state in CoO/Fe/Ag(001) disks

J. Wu,[1] D. Carlton,[2] J. S. Park,[1] Y. Meng,[1,5] E. Arenholz,[3] A. Doran,[3] A.T. Young,[3] A. Scholl,[3] C. Hwang,[4] H. W. Zhao,[5] J. Bokor,[2] and Z. Q. Qiu[1]

[1] Department of Physics, University of California at Berkeley, Berkeley, California 94720, USA

[2] Department of Electrical Engineering and Computer Sciences, University of California at Berkeley, Berkeley, California 94720, USA

[3] Advanced Light Source, Lawrence Berkeley National Laboratory, Berkeley, California 94720, USA

[4] Korea Research Institute of Standards and Science, Yuseong, Daejeon 305-340, Koera

[5] Institute of Phsyics, Chinese Academy of Science, Beijing, P. R. China

In magnetic thin films, a magnetic vortex is a state in which the magnetization vector curls around the center of a confined structure[1]. A vortex state in a thin film disk, for example, is a topological object characterized by the vortex polarity and the winding number[2,3]. In ferromagnetic (FM) disks, these parameters govern many fundamental properties of the vortex such as its gyroscopic rotation[4], polarity reversal[5,6,7], core motion[8], and vortex pair excitation[9]. However, in antiferromagnetic (AFM) disks[10], though there has been indirect evidence of the vortex state through observations of the induced FM-ordered spins in the AFM disk[11,12,13,14], they have never been observed directly in experiment. By fabricating single crystalline NiO/Fe/Ag(001) and CoO/Fe/Ag(001) disks and using X-ray Magnetic Linear Dichroism (XMLD), we show direct observation of the vortex state in an AFM disk of AFM/FM bilayer system. We observe that there are two types of AFM vortices, one of which has no analog in FM structures. Finally, we show that a frozen AFM vortex can bias a FM vortex at low temperature.

Single crystalline NiO/Fe(12nm)/Ag(001) and CoO/Fe(12nm)/Ag(001) films were grown by Molecular Beam Epitaxy (MBE) and patterned into disks using a focused ion beam

(FIB). The FM Fe and AFM NiO and CoO were measured at the Advanced Light Source of Lawrence Berkeley National Laboratory by X-ray Magnetic Circular Dichroism (XMCD) and X-ray Magnetic Linear Dichroism (XMLD). While the XMCD measurement is a standard method, the XMLD measurement on NiO and CoO in our experiment was performed at the Ni L2 edge and Co L3 edge by changing the x-ray linear polarization angle (ϕ) relative to the Fe [001] magnetization axis which is parallel to the NiO or CoO [110] crystalline axis [Fig. 1(a)]. [15] Figure 1 represents a typical CoO XMLD result from CoO(3nm)/Fe(12nm)/Ag(001) with the XMLD signal defined by the so-called L3 ratio (R_{L3}), which is the x-ray absorption intensity at E=778.1 eV divided by the absorption intensity at E=778.9 eV.[15] The L3 ratio follows the expected $\cos^2\phi$ dependence for all CoO thicknesses. Since the L3 ratio under this condition should reach its maximum value for x-ray polarization parallel to the CoO spin axis,[16,17,18] the R_{L3} result in Fig. 1(b) shows that the CoO spins are coupled collinearly to the Fe spins at thinner CoO thickness (d_{CoO}=0.6 nm) and perpendicularly to the Fe spins at thicker CoO thickness (d_{CoO}=3.0 nm). This collinear to 90-degree coupling transition was also reported in NiO/Fe(001) system as a function of NiO thickness.[19] The underlying mechanism of this coupling transition remains unclear up to present and has been a focus of research in this field.

Element-specific magnetic domains were imaged for both the FM Fe and the AFM NiO (CoO) of the bilayer disks at low temperature using Photoemission Electron Beam Microscopy (PEEM). While the FM Fe disks exhibit the expected FM vortices for both circular and square disks, the AFM domain imaging of the NiO and CoO disks reveals unambiguously the existence of the AFM vortex state in the NiO and CoO disks (Fig. 2). It should be emphasized that in addition to the majority AFM-ordered spins (compensated spins), the AFM layer in a AFM/FM bilayer system sometimes could consist of a small amount of FM-ordered spins (uncompensated spins) induced by the FM layer. While the induced FM-ordered spins are located at the AFM/FM interface and resemble the FM layer property, the majority AFM-ordered spins represent the magnetic property of the AFM layer. The AFM vortex state reported in previous works[11,12,13] was actually from the FM-ordered uncompensated spins in the AFM layer at the AFM/FM interface rather than from the majority AFM-ordered compensated spins in the AFM layer. Since the XMLD signal in our work is from the AFM-ordered compensated spins, the NiO and CoO vortices shown in Fig. 2 represent the first direct observation of the AFM vortex state from the AFM-ordered compensated spins, as opposed to the vortex state from the induced FM-ordered

uncompensated spins. The AFM NiO and CoO vortices follow the same pattern of the Fe vortices, showing that the AFM vortex state is imprinted from the FM vortex via the AFM/FM interfacial interaction.[11,12,13] We found that there exist two types of AFM vortices. In thinner NiO (CoO) films, the AFM spins are coupled collinearly with the Fe spins so that the AFM vortex has the conventional structure with the spins curling around the center of the disk in the same manner as the FM vortex [Fig. 2(b)]. However, in thicker NiO (CoO) films, the AFM spins are coupled perpendicularly to the Fe spins to result in an AFM vortex structure with a divergent spin configuration [Fig. 2(c)]. The divergent vortex is forbidden for both a FM disk and for the FM-ordered uncompensated spins in a AFM disk because a divergent FM vortex would produce magnetic charges at the disk boundary to increase the magnetostatic energy. We believe that the divergent vortex is allowed only for the AFM-ordered compensated spins in an AFM disk because the opposite magnetic charges from the two magnetic sublattices of the AFM material cancel each other at the disk boundary.

PEEM measurements are not normally compatible with externally applied fields due to interactions with the photoemitted electrons. However, when the isolation of the bilayer disks from the surrounding Fe thin film is not complete, the disks experience a local magnetic field produced by the surrounding Fe film. This field is mainly localized within the film thus has limited effect on the photoemitted electrons outside the sample. Therefore we can apply the PEEM technique to study the vortex state within the magnetic field of the surrounding Fe film. The strength of the magnetic field from the surrounding Fe film can be estimated as $H = -\int_0^{2\pi} \frac{\cos\theta\sigma(\theta) d_{Fe} r d\theta}{r^2}$, where d_{Fe} is the Fe film thicknesss, r is the radius of the cavity, and $\sigma(\theta)$ is the local magnetic surface charge density. When the surrounding Fe film has a uniform magnetization [Fig. 3(a)], the magnetic surface charge density is given by $\sigma(\theta) = -M_{Fe}\cos\theta$ so that the magnetic field strength can be easily estimated as $H = \frac{M_{Fe} d_{Fe}}{r}\int_0^{2\pi}\cos^2\theta d\theta = \frac{\pi M_{Fe} d_{Fe}}{r}$. For $M_{Fe} = 1700 emu/cm^3$, $d_{Fe} = 12nm$, and $r = 2\mu m$ [Fig. 3(a)], this estimation gives $H \approx 32Oe$. The vortex core position should shift in the transverse direction relative to the magnetic field direction.[20] Fig. 3 shows the Fe PEEM images of the CoO(3nm)/Fe(12nm) disk at room temperature which is above the Néel temperature of the CoO (T_N=291K). Under this condition, the CoO layer is in a paramagnetic state so that it won't bias the Fe disk magnetization in response to the

external magnetic field. As expected, the vortex core of the Fe disk is shifted off-center [Fig. 3(a)] by ~0.5 μm which is about half of the disk radius (R=1 μm). This amount of shift agrees with the experimental observation for a vortex state within a ~30 Oe magnetic field.[21] The magnetic field produced by the surrounding Fe film is reduced by increasing the size of the ring that isolates the disk from the rest of the Fe film. When this field is reduced, the distance by which the vortex core shifts relative to the center of the disk is reduced as expected [Fig. 3(b)].

The CoO/Fe disk was then cooled to 150K to establish the CoO AFM order. Because this cooling took place in the presence of the local magnetic field provided by the surrounding Fe film, the AFM CoO layer is expected to produce an exchange bias[22,23] on the FM Fe layer. If the magnetic field from the Fe magnetization outside the disk could be removed, the exchange bias should have the effect of retaining the Fe vortex in its current off-center state.[12] Since we cannot apply an external magnetic field during the PEEM operation, we can only change the magnetic field to the CoO/Fe disk by changing the domain state of the surrounding Fe film to alter the magnetic surface charge distribution at the boundary of the cavity. In order to change the surrounding Fe film magnetic domains, we sputtered away the CoO overlayer of the surrounding Fe film using focused ion beam sputtering with a careful control of the sputtering time [Fig. 4(a)]. Note that a CoO(3nm)/Fe(2.2nm) film produces an exchange bias field of 480 Oe in the CoO/Fe bilayer with a coercivity of 2000-3000 Oe[15]. The Fe film without the CoO overlayer has a coercivity of only ~50 Oe. Thus we can apply a 50 Oe magnetic field pulse to change the Fe surrounding film domain state without affecting the CoO/Fe bilayer magnetization. A PEEM image confirms that applying a 50 Oe magnetic field pulse in the opposite direction of the Fe magnetization changes the single domain state of the Fe film outside the disk to multi-domain [Fig. 4(b) & (c)]. The 50 Oe external magnetic field was turned off during the PEEM measurement so that only the local magnetic field produced by the surrounding Fe film applies to the CoO/Fe disk during the PEEM measurement. Therefore the local magnetic field produced by the Fe surrounding film to the CoO/Fe disk is reduced from H~32 Oe in Fig. 4(b) to H~0 in Fig. 4(c). Therefore the position of the Fe vortex core would move back towards the center of the disk if there were no exchange bias, however, as shown in Fig. 4(c), the vortex core position of the CoO/Fe disk remains virtually unchanged after switching the outside Fe magnetization. This demonstrates that the exchange bias effect of the CoO vortex on the Fe vortex is retained even after the magnetic field produced by the

surrounding Fe film magnetization has changed from H~32 Oe in Fig. 4(b) to H~0 in Fig. 4(c). This is expected because 32 Oe field is much weaker than the exchange bias field of CoO(3nm)/Fe(12nm) film so the Fe vortex core position should remain unchanged after switching off the 32 Oe local magnetic field. To further verify this effect, we warmed the sample back to room temperature. After the sample temperature is raised above the CoO Néel temperature, as evidenced by the disappearance of the CoO vortex domain [Fig. 4(d)], we observe that the Fe vortex core position moves towards the center of the disk [Fig. 4(d)], showing the diminishing of the exchange bias effect of the CoO layer above its Néel temperature.

Our experimental result not only shows the existence of two types vortex states in the AFM layer of a AFM/FM disk, it also raises many interesting questions for future study. For example, the exchange bias effect in AFM/FM systems has been mostly studied in continuous films. The exchange bias field from an AFM vortex state has not been studied deeply, especially the divergent AFM vortex state. To explore the vortex effect on exchange bias, one would need to measure the FM vortex core position systematically as a function of applied field. Obviously, this kind of study requires different magnetic domain structures of the surrounding Fe film. Applying an AC demagnetization field or a magnetic pulse of different strength could help to realize this. Another new direction could also be developed by imprinting other types of vortices (e.g., antivortex and vortex lattice) from the FM layer into the AFM layer.

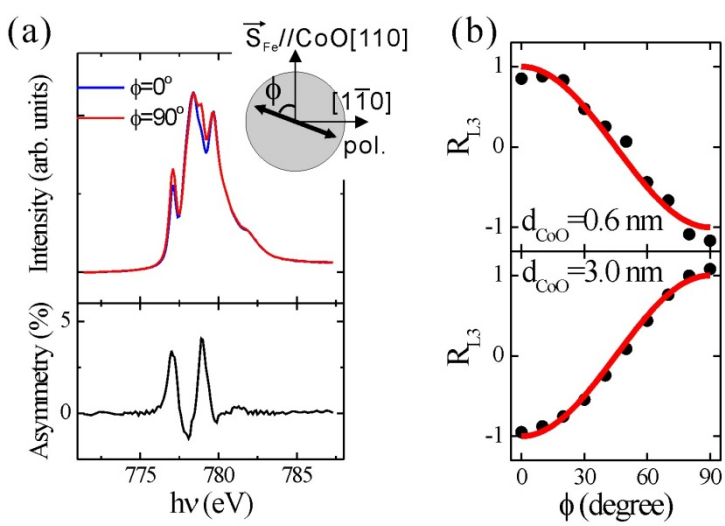

Figure 1: **X-ray Magnetic Linear Dichroism (XMLD) spectra of CoO from CoO/Fe/Ag(001).** (a) The x-ray absorption spectra with the x-ray polarization parallel ($\phi=0^o$) and perpendicular ($\phi=90^o$) to the Fe magnetization direction. The difference between these two absorption spectra shows the XMLD effect. (b) The opposite dependence of the L3 ratio (R_{L3}) of the XMLD on the polarization angle shows that the CoO spins are coupled collinearly (at d_{Co}=0.6 nm) and perpendicularly (at d_{Co}=3.0 nm) to the Fe spins, respectively.

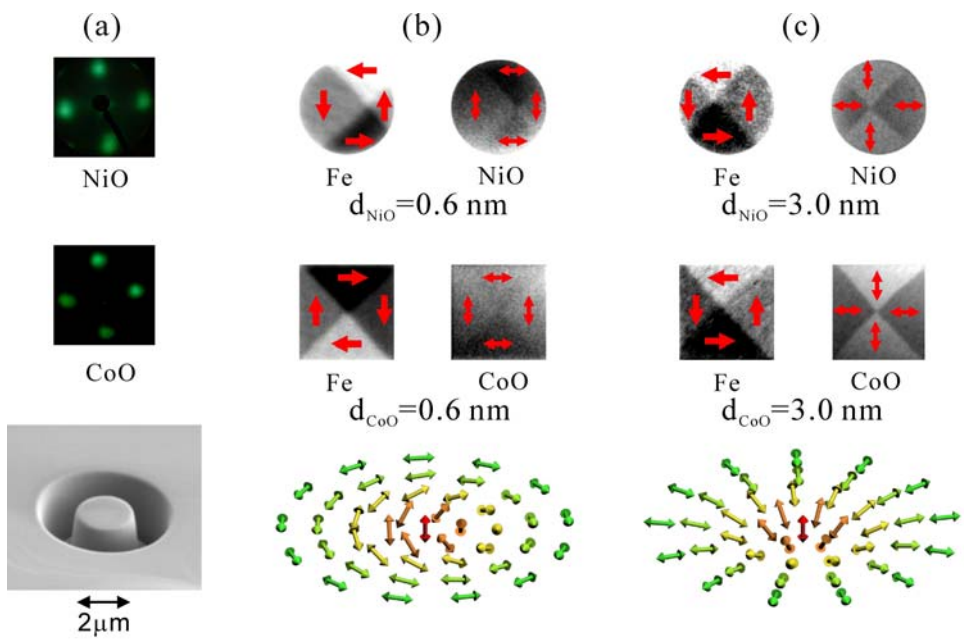

Figure 2: **Element-specific magnetic domain images of NiO/Fe and CoO/Fe disks.** (a) Low Energy Electron Diffraction patterns and Scanning Electron Microscope images of the single crystalline NiO/Fe/Ag(001) and CoO/Fe/Ag(001) disks. The NiO and CoO disks exhibit (b) curling vortices at 0.6 nm NiO and CoO thickness, and (c) divergent vortices at 3.0 nm NiO and CoO thickness. The diameter of the disks is 2 μm, the same as the length of the square patterns. The divergent vortex is forbidden in a FM disk.

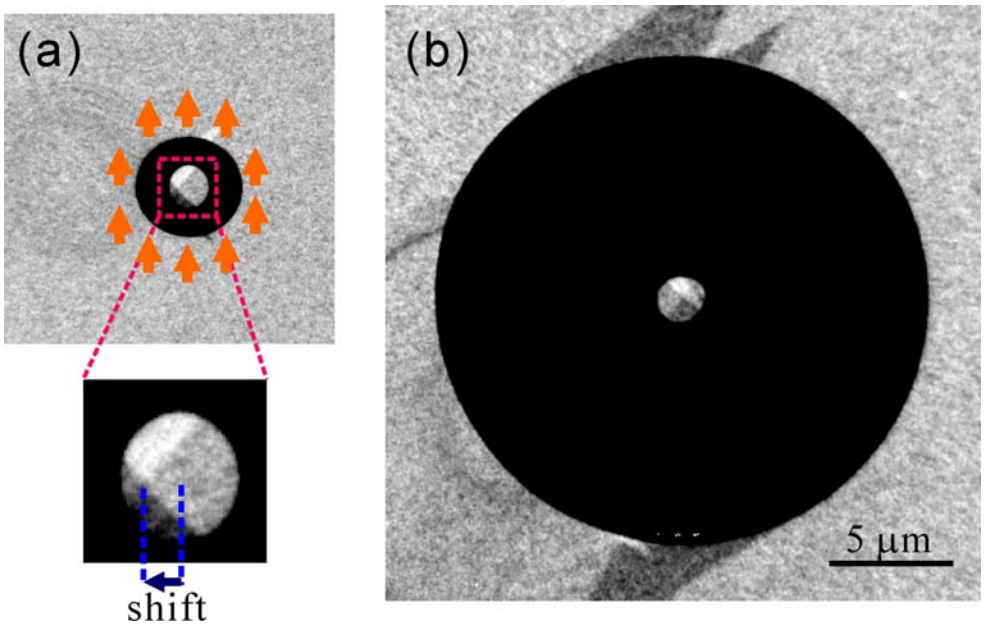

Figure 3: **Fe magnetic domain images taken at room temperature on 2 μm diameter CoO/Fe/Ag(001) disks (The black ring corresponds to the region where the CoO/Fe film is completely removed).** (a) As the diameter of the outer circle is 4 μm, the magnetic field from surrounding Fe film (H~32 Oe) shifts the vortex core by ~0.5 μm. (b) As the diameter of the outer circle is 20 μm, the magnetic field from surrounding Fe film is too weak to shift the vortex core.

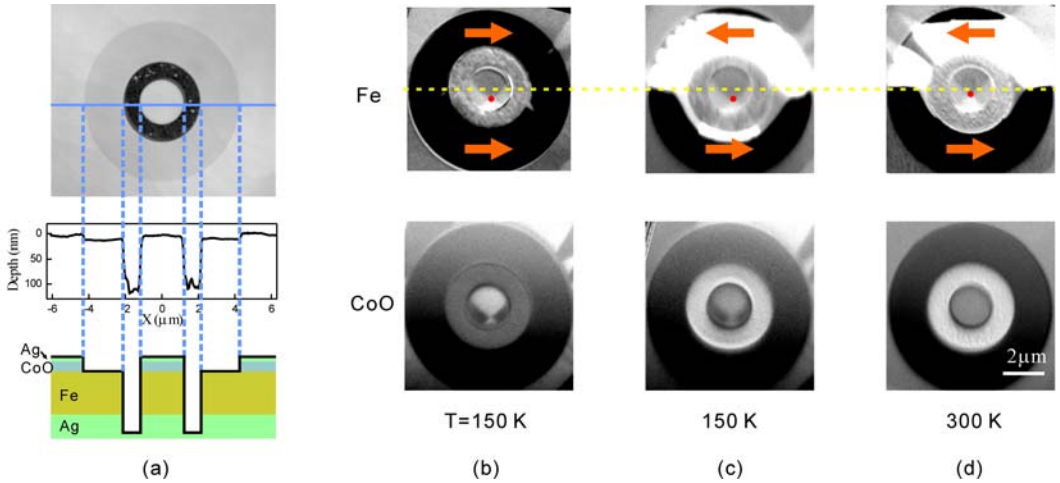

Figure 4: **Magnetic domain images of a 2μm diameter CoO(3nm)/Fe(12nm)/Ag(001) disk under different conditions.** (a) Atomic Force Microscope image, line profile, and schematic drawing of the patterned CoO/Fe/Ag(001) sample. (b) The local magnetic field produced by the surrounding Fe film to the disk (H~ 32 Oe) shifts the vortex core position from the disk center. (b) After applying a 50 Oe magnetic field pulse, the Fe surrounding film changed from single domain state to multi domain state so that the local magnetic field produced by the Fe surrounding film to the disk changed from H~32 Oe to H~0 Oe. The Fe vortex core remains its off-centered position, showing the exchange bias effect from the CoO vortex. (d) After warming up the sample to 300 K (above the CoO Néel temperature), the exchange bias effect vanishes so that the Fe vortex core moves to the center position of the disk.

Method

NiO/Fe/Ag(001) and CoO/Fe/Ag(001) films were grown epitaxially by Molecular Beam Epitaxy in an ultrahigh vacuum system with a base pressure of $2x10^{-10}$ Torr. The Fe film was grown by evaporating Fe from a thermal crucible. The NiO and CoO films were grown by evaporating the Ni and Co in an oxygen environment of 10^{-6} Torr. The typical evaporation rate is ~1Å/min. Low Energy Electron Diffraction results show that single crystalline NiO/Fe and CoO/Fe films were formed with the NiO [110] and CoO [110] axes

parallel to the Fe [100] and Ag [110] axes (Fig. 2). The formation of single crystalline NiO and CoO ensures a nonzero XMLD signal from the NiO and CoO films. After covering the film with a 2nm thick Ag protection layer, the films were taken out of the vacuum system and patterned using focused ion beam patterning (Fig. 2). The sample was measured at both the beamline 4 and the PEEM-3 station of the Advanced Light Source at the Lawrence Berkeley National Laboratory. In the PEEM-3 station, an electromagnet near the sample holder allows the application of an external magnetic field pulse to the sample to change the magnetic domain state of the sample. However, the external magnetic field must be turned off during the PEEM measurement because the Lorentz force on the photoemitted electrons by the external magnetic field prohibits PEEM image acquisition.

For the FM Fe disks, X-ray Magnetic Circular Dichroism (XMCD) was used to image the Fe domain at the Fe L3 edge absorption peak. For AFM NiO and CoO disks, X-ray Magnetic Linear Dichroism (XMLD) was used to image the NiO and CoO domain at the Ni L2 and Co L3 edge absorption peaks. XMCD measurements on the Ni and Co L-edge were also performed. The absence of Ni and Co XMCD signal confirms that the XMLD signal is from the antiferromagnetically ordered compensated spins. For the XMLD spectrum measurement (Fig. 1), the Fe magnetization was aligned to its easy magnetization [100] axis which is parallel to the NiO or CoO [110] axis. Under this condition, the XMLD signal should reach its maximum value when the x-ray polarization axis coincides with the NiO and CoO spin axes. A detailed description can be found in Ref. 15.

Acknowledgement

This work was supported by National Science Foundation DMR-0803305, U.S. Department of Energy DE-AC02-05CH11231, KICOS through Global Research Laboratory project, Chinese Education Department, and Western Institute of Nanolectronics (WIN).

Author contributions

J. W. and Z. Q. Qiu designed and performed experiments, analyzed data and wrote the paper; D. C and J. B. patterned the disks and wrote the paper; J.S.P., Y.M., E.A., A.D., A.T.Y., A.S., C.H. and H.W.Z. performed the x-ray measurements and discussion.

Additional information

Correspondence and request for materials should be addressed to Z. Q. Q.

References:

1. Shinjo, T., Okuno, T., Hassdorf, R., Shigeto, K. and Ono, T. Magnetic Vortex Core Observation in Circular Dots of Permalloy. Science **289**, 930-932 (2000).

2. Tretiakov, O. A. and Tchernyshyov, O. Vortices in thin ferromagnetic films and the skyrmion number. Phys. Rev. B **75**, 012408 (2007).

3. Yu, X. Z., Onose, Y., Kanazawa, N., Park, J. H., Han, J. H., Matsui, Y., Nagaosa, N. and Tokura, Y., Real-space observation of a two-dimensional skyrmion crystal. Nature **465**, 901-904 (2010).

4. Choe, S.-B., Acremann, Y., Scholl, A., Bauer, A., Doran, A., Stohr, J. and Padmore, H. A. Vortex Core-Driven Magnetization Dynamics. Science **304**, 420-422 (2004).

5. Van Waeyenberge, B., Puzic, A., Stoll, H., Chou, K. W., Tyliszczak, T., Hertel, R., Fähnle, M., Brückl, H., Rott, K., Reiss, G., Neudecker, I., Weiss, D., Back, C. H. and Schütz, G. Magnetic vortex core reversal by excitation with short bursts of an alternating field. Nature **444**, 461-464 (2006).

6. Hertel, R., Gliga, S., Fähnle, M. & Schneider, C. M. Ultrafast nanomagnetic toggle switching of vortex cores. Phys. Rev. Lett. **98**, 117201 (2007).

7. Yamada, K., Kasai, S., Nakatani, Y., Kobayashi, K., Kohno, H., Thiaville, A., and Ono, T. Electrical switching of the vortex core in a magnetic disk. Nature Materials **6**, 270-273 (2007).

8. Vansteenkiste, A., Chou, K. W., Weigand, M., Curcic, M., Sackmann, V., Stoll, H., Tyliszczak, T., Woltersdorf, G., Back, C. H., Schütz G. and Van Waeyenberge, B. X-ray imaging of the dynamic magnetic vortex core deformation. Nature Physics **5**, 332-334 (2009).

9. Buchanan, Kristen S., Roy, Pierre E., Grimsditch, Marcos, Fradini, Frank Y., Guslienko, Konstantin Yu. Bader, Sam D. and Novosad, Valentyn. Soliton-pair dynamics in patterned ferromagnetic ellipses. Nature Physics **1**, 172-176 (2005).

10. Senthil, T., Vishwanath, A., Balents, L., Sachdev, S. and Fisher, M. P. A. Deconfined Quantum Critical Points. Science **303**, 1490-1494 (2004).

11. Sort, J., Buchanan, K. S., Novosad, V., Hoffmann, A., Salazar-Alvarez, G., Bollero, A., Baró, M. D., Dieny, B., and Nogués, J. Imprinting Vortices into Antiferromagnets. Phys. Rev. Lett. **97**, 067201 (2006).

12. Hoffmann, Axel, Sort, Jordi, Buchanan, Kristen S. and Nogués, Josep Exchange-Biased Magnetic Vortices, IEEE Transactions on Magnetics **44**, 1968-1973 (2008).

13. Salazar-Alvarez, G., Kavich, J. J., Sort, J. Mugarza, A., Stepanow, S., Potenza, A., Marchetto, H., Dhesi, S. S., Baltz, V., Dieny, B., Weber, A., Heyderman, L. J., Nogués, J. and Gambardella, P. Direct evidence of imprinted vortex states in the antiferromagnet of exchange biased microdisks. Appl. Phys. Lett. **95**, 012510 (2009).

14. Tanase, M., Petford-Long, A. K., Heinonen, O., Buchanan, K. S., Sort, J., and Nogués, J. Magnetization reversal in circularly exchange-biased ferromagnetic disks. Phys. Rev. B **79**, 014436 (2009).

15. Wu, J., Park, J. S., Kim, K., Arenholz, E., Liberati, M., Scholl, A., Wu, Y. Z., Hwang, Chanyong, and Qiu Z. Q. Direct Measurement of rotatable and Frozen CoO Spins in Exchange Bias System of CoO/Fe/Ag(001). Phys. Rev. Lett. **104**, 217204 (2010).

16. Arenholz, E., van der Laan, G., Chopdekar, R. V., and Suzuki, Y. Angle-Dependent Ni^{2+} X-Ray Magnetic Linear Dichroism: Interfacial Coupling Revisited. Phys. Rev. Lett. **98**, 197201 (2007).

17. van der Laan, G., Arenholz, E., Chopdekar, R. V., and Suzuki, Y., Influence of crystal field on anisotropic x-ray magnetic linear dichroism at the Co^{2+} $L_{2,3}$ edges. Phys. Rev. B **77**, 064407 (2008).

18. Nevidomskyy, A. H., Scheiber, C., Sénéchal, D., and Tremblay, A.-M. S. Magnetism and d-wave superconductivity on the half-filled square lattice with frustration. Phys. Rev. B **77**, 064427 (2008).

19. Finazzi, M., Brambilla, A., Biagioni, P., Graf, J., Gweon, G.-H., Scholl, A., Lanzara, A., and Duo, L. Interface Coupling Transition in a Thin Epitaxial Antiferromagnetic Film Interacting with a Ferromagnetic Substrate. Phys. Rev. Lett. **97**, 097202 (2006).

20. Guslienko, K. Yu., Novosad, V., Otani, Y., Shima, H. and Fukamichi, K. Field evolution of magnetic vortex state in ferromagnetic disks. Appl. Phys. Lett. **78**, 3848-3850 (2001).

21. Uhlig, T., Rahm, M., Dietrich, C., Hollinger, R., Heumann, M., Weiss, D., and Zweck, J. Shifting and Pinning of a Magnetic Vortex Core in a Permalloy Dot by a Magnetic Field. Phys. Phys. Lett. **95**, 237205 (2005).

22. Meiklejohn, W. H. and Bean, C. P. New Magnetic Anisotropy. Phys. Rev. **102**, 1413-1414 (1956).

23. Nogues, J. and Schuller, I. K. Exchange bias. J. Magn. Magn. Mater. **192**, 203-232 (1999).

LEGAL DISCLAIMER

This document was prepared as an account of work sponsored by the United States Government. While this document is believed to contain correct information, neither the United States Government nor any agency thereof, nor The Regents of the University of California, nor any of their employees, makes any warranty, express or implied, or assumes any legal responsibility for the accuracy, completeness, or usefulness of any information, apparatus, product, or process disclosed, or represents that its use would not infringe privately owned rights. Reference herein to any specific commercial product, process, or service by its trade name, trademark, manufacturer, or otherwise, does not necessarily constitute or imply its endorsement, recommendation, or favoring by the United States Government or any agency thereof, or The Regents of the University of California. The views and opinions of authors expressed herein do not necessarily state or reflect those of the United States Government or any agency thereof or The Regents of the University of California.